IEEE Access
Multidisciplinary | Rapid Review | Open Access Journal

Received September 17, 2021, accepted September 28, 2021, date of publication October 4, 2021, date of current version October 12, 2021.

Digital Object Identifier 10.1109/ACCESS.2021.3117295

Lateral Stability Control of a 4-Wheel Independent Drive Electric Vehicle Using the Yaw Moment Contour Line Concept

IN-GYU JANG[1], SEUNG-HAN YOU[2], SUNG-HO HWANG[1], AND WANKI CHO[2]
[1]School of Mechanical Engineering, Sungkyunkwan University, Suwon 16419, South Korea
[2]School of Mechanical Engineering, Korea University of Technology and Education, Cheonan 31253, South Korea

Corresponding author: Wanki Cho (wkcho@koreatech.ac.kr)

This work was supported in part by Mando Halla Company, in part by the National Research Foundation of Korea (NRF) Grant by the Korean Government through MSIT under Grant NRF-2021R1F1A1050200, and in part by the Technology Innovation Program (or Industrial Strategic Technology Development Program—Development of the Core System Technology for Hyper-Safe Driving Platform) by the Development of Hyper-Safe Driving Platform Based on Cooperative Domain Control through the Ministry of Trade, Industry and Energy (MOTIE), South Korea, under Grant 20015831.

ABSTRACT This paper describes a new algorithm that independently manages braking and driving forces to improve the lateral stability of a vehicle equipped with independent drive motors on all wheels. In a similar way to previous research, the proposed algorithm controls yaw rate to improve lateral stability. However, unlike in previous research that only used differential braking, our algorithm controls both driving and braking forces on all four wheels independently to achieve the target yaw rate. The core contribution of this paper is the distribution logic that determines the braking and driving forces to apply at each wheel. To develop this distribution logic, we introduce the concept of yaw moment contour line. Using this concept, the optimal distribution strategy can be derived by considering yaw moment control performance, lateral movement performance, and deceleration minimization performance in eight different driving situations. Based on this strategy, we design a lateral stability control algorithm that is made up of a target yaw rate, a yaw moment controller, and a distributor. Simulations were performed to investigate the performance of the proposed algorithm using MATLAB/Simulink and the CarSim vehicle dynamics software. The simulation results show that the proposed control algorithm improves vehicle motion in terms of yaw rate tracking, lateral movement, and minimization of deceleration.

INDEX TERMS Electric vehicle, 4-wheel independent drive, yaw moment contour line, lateral stability, optimal distribution.

I. INTRODUCTION

Recently, the electric vehicle market has expanded due to the EU's strict CO_2 regulations and the emergence of an innovative leading company, Tesla. The Electricity Vehicle Outlook 2020 published by Bloomberg New Energy Finance predicts that sales of electric vehicles will surge between 2025 and 2030, and by 2040, electric vehicles will account for 58% of new car sales and 33% of global cars [1]. The most important issue in a situation where electric vehicles are in the limelight and the number of mass-produced vehicles is increasing is how far they can travel on a single charge. To solve this issue, electric vehicles are currently equipped with many batteries. This increases the weight of the vehicle significantly. Also, since batteries are widely mounted under the vehicle's body for the weight distribution, the moment of inertia becomes very large. The large moment of inertia decreases the vehicle's turning performance, and it is very difficult to re-stabilize the vehicle when it is in an unstable state. One of the ways to solve this problem is the development of a high-performance electric vehicles equipped with independent drive motors at each wheel. This system has the advantage of giving a lot of freedom in terms of motion control because it becomes possible to independently control braking and driving forces at each wheel. Research on stability control for these kinds of electric vehicles with four-wheel independent drive systems is needed.

The associate editor coordinating the review of this manuscript and approving it for publication was Christopher H. T. Lee.

Previous studies over the past ten years on independent drive electric vehicles have mainly focused on how to utilize the independent wheel torque control characteristics to maintain stability of the vehicle [2]–[8]. Kang *et al.* proposed a driving control algorithm for maneuverability, lateral stability, and rollover prevention in 4WD electric vehicles using an optimization-based control allocation strategy [2]. Chen. *et al.* designed an optimization strategy to improve the handling and stability of electric vehicles with four in-wheel independent-drive motors (4WIDEV) [3]. The hierarchical coordination control approach for differential drive assist steering (DDAS) and the vehicle stability control(VSC) was introduced by Wang. *et al* [4]. Nam *et al.* proposed a method that uses lateral tire force sensors to estimate vehicle sideslip angle and improve vehicle stability for in-wheel motor-driven electric vehicles (IWM-EVs) [5]. A novel control strategy to improve the stability performance for four-wheel independent drive electric vehicles in critical cornering was established by introducing the supervision mechanism for yaw moment control for yaw moment control and slip ratio regulation simultaneously [6]. In order to improve the steering stability for a four in-wheel motor independent-drive electric vehicle (4MIDEVs) on a road with varying adhesion coefficient, Hou *et al.* presents a hierarchical electronic steering control strategy. This method consists of the upper level controller, which determines the yaw moment to control the yaw rate and side slip angle, and the lower level controller, which calculates the optimal braking/driving torque at each wheel [7]. Kim *et al.* investigated a VSC algorithm for 4WD hybrid EVs that uses regenerative braking in the rear motor in addition to hydraulic brakes [8]. Further studies were conducted that included not only independent drive but also active steering control [9]–[14]. Shuai *et al.* proposed an optimal integration method of a four-wheel independent drive system and an active front steering system to improve vehicle lateral stability [9], [10]. An integrated optimal dynamics control of four-wheel driving and four-wheel steering (4WD4WS) electric ground vehicle was developed by using an LQR controller and optimal distribution considering a stable margin at each wheel [11]. To improve the handling and maneuverability of four-wheel steer (4WS) and in-wheel motor driven electric vehicle (EV) in which the mechanical properties of tires are unknown, an optimal coordinated control combining active rear wheel steering (ARS) and direct yaw moment control (DYC) in the form of active drive torque distribution is proposed by Wang *et al.* [12]. Several studies have proposed an optimization method proportional to the load at each wheel in the distribution of the four-wheel drive system and the front and rear wheel steering systems [13], [14]. In addition to these, many studies have been conducted that integrate differential braking and active steering system for the vehicle lateral stability control, although not using a four-wheel independent drive system [15]–[18]. There have been the studies that integrated differential braking and active front steering system [15]–[17] and the study that integrated differential braking and rear wheel steering system [18]. Most of these previous studies calculate the target yaw moment to track the target yaw rate, and determine the braking and driving force at each wheel through an optimization method to generate this target yaw moment. The object of the optimization is to minimize the control inputs and the error between the yaw moment generated by these control inputs and the target yaw moment. To minimize the control inputs, the cost function and constraint of the optimization are determined so that the optimized control inputs (braking/driving force) of each wheel are proportional to the load and controllable margin of that wheel. That is, it is assumed that the yaw moment generation effect by the braking or driving force is proportional to the load on the wheel. However, depending on the driving situation, the yaw moment generation effects by the braking and driving force applied to each wheel can be different regardless of the wheel load. For example, in the case of conventional ESC that uses only differential braking, the unstable states of the vehicle are classified into understeer (US) and oversteer (OS). Due to the non-linearity of tire force, during US, braking at the rear-inner wheel is most effective for stability, and during OS, braking at the front-outer wheel [19]. Another problem here is how to recognize OS and US. It is possible to recognize US and OS in steady-state cornering such as during a J-turn or circular turning, but it is difficult to determine in transient driving situations such as during a single lane change (SLC) or slalom. To solve these problems, new control logic that provides lateral stability using independent braking and driving forces at each wheel is proposed in this paper. This control logic has the same structure as the previous studies that calculates the target yaw moment to track the target yaw rate and determines the braking and driving force at each wheel through optimization method. The difference from previous studies is that the yaw moment control performance, lateral movement performance, and deceleration minimization performance are considered, not the wheel load when determining the braking and driving force at each wheel through the optimization method. To do this, this paper introduces a new concept called the yaw moment contour line and proposes optimal distribution strategies for all driving situations using this concept. All driving situations can be defined as eight types according to the lateral forces on the front and rear wheels and the target yaw moment. By applying the concept of the yaw moment contour line, the optimal distribution strategies for each driving situation are determined by considering yaw moment control performance, lateral movement performance, and deceleration minimization performance. Using the optimal distribution strategies, we develop the control algorithm consisting of a target yaw rate, Mz controller, and distributor. To evaluate the proposed algorithm, simulations using Carsim and Matlab/Simulink were carried out to confirm that the algorithm improves yaw rate control, lateral movement, and deceleration minimization. The main contribution of this paper is to establish the optimal distribution strategy by applying the new concept called yaw moment contour line.

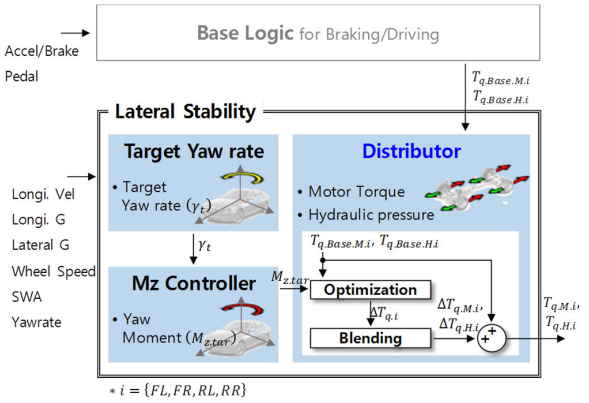

FIGURE 1. Control architecture.

In order to develop the algorithm, information on the tire-road friction coefficient, vehicle speed, lateral and vertical tire forces was required, how these values are known in our method will not be discussed in detail in this paper because these signals can be estimated using one of the many estimators proposed by previous researchers [20]–[22]. In addition to these vehicle signals, vehicle parameters such as inertia and mass, which are important information for securing the robustness of the control algorithm, can also be estimated through the previous study [23].

II. CONTROL ARCHITECTURE

Fig. 1 shows the architecture of the proposed lateral stability control algorithm. This algorithm receives the wheel speed, yaw rate, longitudinal, lateral acceleration, and the driver's steering input, it then outputs the required motor torque and hydraulic friction braking torque for each wheel. The base logic for braking/driving module receives the driver's brake and accelerator pedal signals then calculates the motor torque ($T_{q.Base.M.i}$) and hydraulic braking torque ($T_{q.Base.H.i}$) to be applied at each wheel for the desired deceleration or acceleration of the vehicle. These control values are calculated in consideration of fuel economy and traction performance rather than lateral stability. The lateral stability control module consists of the target yaw rate, Mz controller, and distributor. The target yaw rate (γ_t) is determined based on vehicle velocity and the driver's steering angle. To track this target motion, the Mz controller calculates the target yaw moment ($M_{z.tar}$), which is the control value for the sprung mass of the vehicle. Finally, the distributor calculates the final motor torque ($T_{q.M.i}$) and the hydraulic braking torque ($T_{q.H.i}$) required to generate the target yaw moment in consideration of the control signals being generated by the base logic for braking/driving module. The optimization module in the distributor calculates the additional torque required ($\Delta T_{q.i}$) at each wheel to generate the target yaw moment. These are then distributed as motor torque ($\Delta T_{q.M.i}$) and hydraulic braking torque ($\Delta T_{q.H.i}$) through the blending module and the final control values ($T_{q.M.i}$ and $T_{q.H.i}$) are determined by adding the motor torque and the hydraulic braking torque of the base logic for braking/driving module. Next, each module will be described in detail. Since the goal of this paper is to develop a control algorithm for improving lateral stability, we do not discuss the base logic of braking/driving module as this is not related to lateral stability. The target yaw rate and Mz controller of the lateral stability control module will be briefly introduced because the results of previous studies are used.

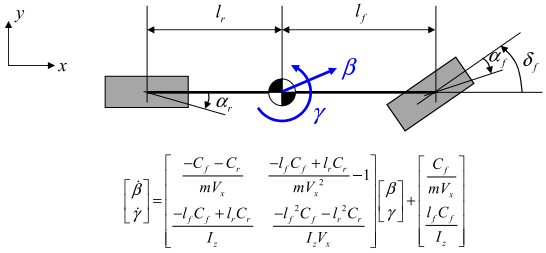

FIGURE 2. Bicycle model and equation.

III. TARGET YAW RATE & MZ CONTROLLER

Since the target yaw rate and Mz controller are the same as those in previous research, detailed descriptions will be omitted. The bicycle model is used to calculate the target yaw rate [17]. Fig. 2 shows the bicycle model and its equations. This model is a two-degrees-of-freedom model that consists of the yaw rate (γ) and sideslip angle (β), and assumes that the longitudinal velocity is constant.

Using this model, it is possible to calculate the steady state yaw rate for the driver's steering angle ($\dot{\gamma} = 0, \dot{\beta} = 0$).

$$\gamma_{ss} = \frac{1}{1 - \frac{m(l_f \cdot C_f - l_r \cdot C_r)V_x^2}{C_f \cdot C_r (l_f + l_r)^2}} \frac{v_x}{l_f + l_r} \delta_f \tag{1}$$

To avoid a large target yaw rate that exceeds the tires cornering capability, the yaw rate is constrained as follows:

$$\gamma_{ss.Lim} = \text{sign}\,(\gamma_{ss}) \cdot \min\left(|\gamma_{ss}|, \frac{\mu g}{V_x}\right) \tag{2}$$

As the yaw rate from (2) will have the same phase as the steering angle, a phase difference from the actual yaw rate will occur. To solve this problem, the final target yaw rate is determined as follows by imposing a certain phase delay on the result from (2).

$$\gamma_t = \frac{1}{1 + \tau s} \gamma_{ss.Lim} \tag{3}$$

The Mz controller calculates the target yaw moment needed to track the target yaw rate. This module is simply designed using PD control.

$$M_{z.tar} = K_p \cdot (\gamma_t - \gamma) + K_d \cdot (\dot{\gamma}_t - \dot{\gamma}) \tag{4}$$

IV. DISTRIBUTOR

The distributor calculates motor torque and hydraulic braking torque for each wheel to achieve the target yaw moment. Driving situations are classified into eight categories according to the signs of the target yaw moment, front-wheel lateral forces, and rear-wheel lateral forces, we then introduce a new concept called the yaw moment contour line to derive

an optimal distribution strategy for every situation. Based on this concept, the optimal distribution strategy is derived by analyzing yaw moment control performance, lateral movement performance, and deceleration minimization in each situation. Fig. 3 shows the architecture of the distributor. It is composed of an optimization module and a blending module. In the optimization module, the optimal torque to be applied at each wheel to achieve the target yaw moment is determined based on the established distribution strategy and the torque limit of the motors. This torque is distributed as motor torque and hydraulic braking torque through the blending module. We will now describe the distributor in detail. First, the concept of the yaw moment contour line and the optimal distribution strategy based on this concept are described. In addition, the optimization module and the blending module are explained.

A. YAW MOMENT CONTOUR LINE

The yaw moment contour line is a line that represents the possible longitudinal and lateral tire forces that generate the same yaw moment, as shown in Fig. 4. Looking at Fig. 4, the black circle represents the friction circle of each wheel and the dotted black lines represent the yaw moment contour lines. The same yaw moment is generated if the resultant force from the longitudinal and lateral tire forces are located on the same yaw moment contour line. As shown on the right side of Fig.4, if the resultant forces for the longitudinal and lateral tire forces are located on the red line, it can be seen that the generated yaw moment is $\Delta F \times L$. Also, it can be seen that when the yaw moment contour line moves to the left based on the center of gravity of the vehicle, the generated yaw moment sees a positive increase, in the opposite case, it sees a negative increase. Using this concept, the optimal distribution strategy for each driving situation is established in the next section.

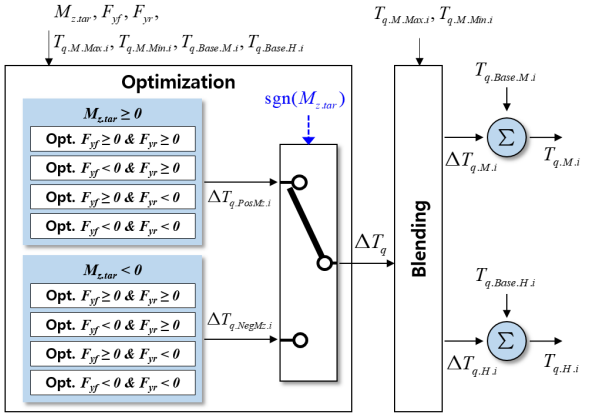

FIGURE 3. Architecture of the distributor.

B. OPTIMAL DISTRIBUTION STRATEGY

In this section, the optimal distribution strategy for each driving situation is established using the yaw moment contour lines described in the previous section. In order to optimally distribute forces to each wheel, the following three distribution optimization goals are established in this paper.

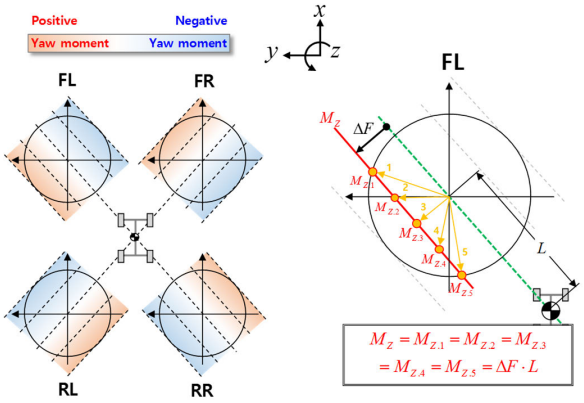

FIGURE 4. Concept of yaw moment contours.

- Yaw moment control performance
  The purpose of this paper is to improve lateral stability through yaw rate control, so yaw rate should be controlled efficiently. That is, a large (yaw moment control) effects must be obtained with small control values (motor torque and hydraulic braking torque).
- Lateral movement performance
  Due to the non-linear characteristics of tires, when longitudinal forces such as braking or driving forces are applied during cornering, the magnitude of the lateral tire force changes. Using this principle, we can analyze lateral movement performance. Lateral movement performance is a criterion for determining how much a vehicle has moved to the left (right) side when turning left (right), it can be determined by looking at whether the lateral tire force has increased or decreased. If the torque applied for yaw rate control increases the lateral tire force in the turning direction, it can be said that lateral movement performance is good.
- Deceleration minimization performance
  In the case of the conventional ESC systems, the desired yaw moment is generated by differential braking. However, differential braking leads to significant longitudinal decelerations and pitch motion of the vehicle body. These could be sensed by the driver and thus lead to a degradation of ride comfort. Therefore, it is necessary to minimize deceleration that is not intended by the driver.

Among the three goals mentioned above, the optimal distribution strategy can be established based on the yaw moment control performance and lateral movement performance. The deceleration minimization performance is reflected in the design of the optimal distribution algorithm. The yaw moment contour lines in Fig. 4 show that the yaw moment control performance by braking or driving forces depends on tire lateral force signs. Therefore, optimal distribution strategies are established for eight driving situations according to the signs of the target yaw moment, front-wheel lateral forces, and rear-wheel lateral forces. This paper does not mention all eight driving situations, but only deals with four cases where the target yaw moment has a positive value. This is because when the yaw moment is negative, the same method as with

the positive yaw moment is applied. In addition, since it is a situation that requires vehicle stability control, it is assumed that all tire forces exist in the friction circle. Then, from now on, we will mention the optimal distribution strategy for the four cases where the target yaw moment is positive.

1) CASE 1: $M_{z,tar} > 0, F_{yf} > 0, F_{yr} > 0$

Fig. 5 shows the driving situation and the control performance analysis result for Case 1. The purple, black, and gray dots represent the tire forces under acceleration, constant speed, and deceleration, respectively. Since the lateral forces of the front and rear wheels are both positive, this represents a left turn. In addition, since the target yaw moment direction is counterclockwise, additional rotation to the left is required. To generate the target yaw moment, the left wheels (FL and RL) need braking and the right wheels (FR and RR) need drive. The purple, black, and gray arrows indicate the travel path of the tire force due to the yaw moment control. As the direction of the arrow and the direction of the yaw moment contour line become closer to the vertical, the yaw moment control performance becomes more effective. That is, a large yaw moment can be generated by a small change in tire force. In the case of the FL wheel, if the current acceleration state (purple dot), the tire force moves in the direction of the purple arrow (FL Region 1) by braking control. In this situation, the direction of travel of the tire force is nearly perpendicular to the direction of the yaw moment contour line, so the yaw moment control performance is effective. As the lateral tire force increases to the left, the lateral movement performance also becomes better. However, when the braking force increases and passes the black point (FL Region 2), the direction of travel of the tire force (black arrow) becomes parallel to the direction of the yaw moment contour line, and the lateral force decreases. In other words, the yaw moment control performance and the lateral movement performance deteriorate. If the tire force passes the gray point as a result of an increase in braking control, the yaw moment control has the opposite effect. In the case of the analysis on the FR wheel, unlike the FL, the analysis starts from the deceleration situation (gray dot). As the tire force moves in the direction of the gray arrow (FR Region 1), both the yaw moment control performance and the lateral movement performance are good. However, if the tire force passes through the black point due to an increase in the required driving force (FR Region 2), the yaw moment control performance and the lateral movement performance deteriorate, in a similar way to the FL. In the case of the RL wheel, the yaw moment control performance is not good under acceleration (purple dot), but it can be seen that the lateral force increases to the left. When the braking force increases and passes the black point, the lateral force decreases but the yaw moment control performance improves. In this case, it can be seen that the larger the braking force is, the better the yaw moment control performance is. The analysis for the RR wheel is not mentioned as it is similar to that of the RL wheel.

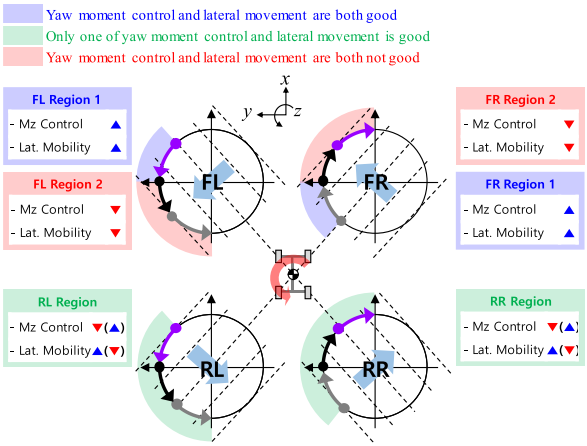

FIGURE 5. Control performance analysis result for Case 1.

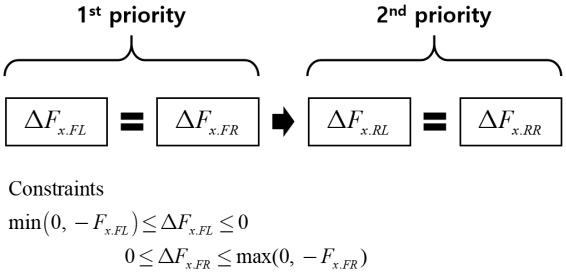

FIGURE 6. Optimal distribution strategy for Case 1.

Based on the above analysis results, the optimal distribution strategy for Case 1 is established as shown in Fig. 6. $\Delta F_{x.i}$ $(i = FL, FR, RL, RR)$, $F_{x.FL}$ and $F_{x.FR}$ represent the required control values to be distributed to each wheel, and the longitudinal tire forces of the FL and FR wheels, respectively. As shown in the figure, the target yaw moment is first achieved by distributing braking force to the FL wheel and driving force to the FR wheel. However, since the FL braking force and FR driving force are only effective in Region 1, constraints on the wheel forces are required. When the braking and the driving of the front wheels alone is not enough to generate the target yaw moment, the insufficient yaw moment is achieved by distributing braking force to the RL wheel and driving force to the RR wheel.

2) CASE 2: $M_{z,tar} > 0, F_{yf} < 0, F_{yr} > 0$

Case 2 is where the lateral forces on the front and rear wheels are negative and positive, respectively, this situation occurs just after steering clockwise to change the direction of a vehicle that was turning left to turn right. Since the target yaw moment direction was counterclockwise, it is necessary to transition into the right turn slowly. In this case, since the signs of the lateral forces on the front and rear wheels are opposite, an analysis of lateral movement performance is not carried out. Fig. 7 shows the driving situation and control performance analysis results for Case 2. For all four wheels, we can see that the direction of travel of the tire force is effective for yaw moment control performance. Therefore, in Case 2, the yaw moment is equally distributed to all wheels.

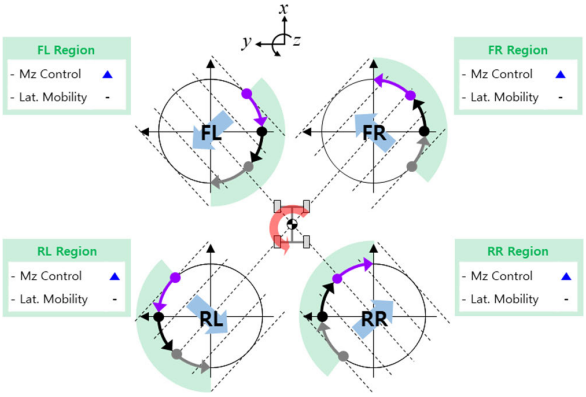

FIGURE 7. Control performance analysis result for Case 2.

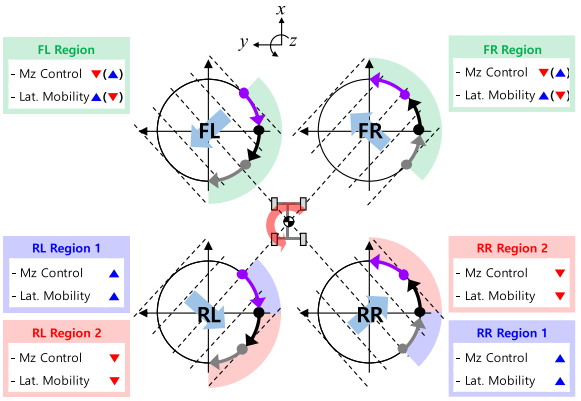

FIGURE 8. Control performance analysis result for Case 3.

3) CASE 3: $M_{z,tar} > 0, F_{yf} < 0, F_{yr} < 0$

In Case 3, since the lateral forces on the front and the rear wheels are both negative this represents a right turn while the target yaw moment direction is counterclockwise, so it is necessary to suppress the right turn. Fig. 8 shows the driving situation and control performance analysis results for Case 3. It can be seen that the analysis results for the front and rear wheels have changed compared to Case 1. Therefore, the optimal distribution strategy for Case 3 can be expressed as shown in Fig. 9.

4) CASE 4: $M_{z,tar} > 0, F_{yf} > 0, F_{yr} < 0$

Case 4 is the case where the lateral forces of the front and rear wheels are positive and negative, respectively, and the driving situation is just after turning the steering counterclockwise to change the direction of a vehicle that was turning right to turn left. The direction of the target yaw moment is counterclockwise while the vehicle has already achieved a counterclockwise yaw moment, it simply needs to transition to a faster left turn. For the same reasons as in Case 2, the lateral movement performance is not analyzed. Fig. 10 shows the driving situation and the control performance analysis results for Case 4. It can be seen that the yaw moment control performance of all 4 wheels is not good except for in Region 1. Therefore, the optimal distribution strategy for Case 4 is to first distribute the yaw moment to the wheel where the current tire force is in Region 1. If this is still insufficient to generate the target yaw moment, the insufficient yaw moment is achieved by distributing appropriate forces to all wheels. However, in Region 2, the yaw moment control performance is not good, and in this situation, if the control value is increased further, it has the opposite effect on performance. Therefore, the yaw moment should only be distributed before this opposite effect region (gray arrow) is reached.

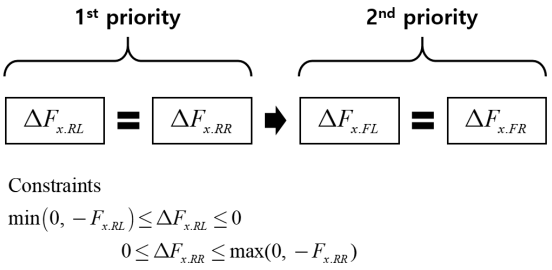

FIGURE 9. Optimal distribution strategy for Case 3.

TABLE 1. Optimal distribution strategies for eight driving situations.

Pos. $M_{z.tar}$ (+)	Case 1 (F_{yf}+, F_{yr}+)	$\Delta F_{x.FL} = \Delta F_{x.FR} \rightarrow \Delta F_{x.RL} = \Delta F_{x.RR}$ $min(0, -F_{x.FL}) \le \Delta F_{x.FL} \le 0$ & $0 \le \Delta F_{x.FR} \le max(0, -F_{x.FR})$
	Case 2 (F_{yf}-, F_{yr}+)	$\Delta F_{x.FL} = \Delta F_{x.FR} = \Delta F_{x.RL} = \Delta F_{x.RR}$
	Case 3 (F_{yf}-, F_{yr}-)	$\Delta F_{x.RL} = \Delta F_{x.RR} \rightarrow \Delta F_{x.FL} = \Delta F_{x.FR}$ $min(0, -F_{x.RL}) \le \Delta F_{x.RL} \le 0$ & $0 \le \Delta F_{x.RR} \le max(0, -F_{x.RR})$
	Case 4 (F_{yf}+, F_{yr}-)	$\Delta F_{x.FL} = \Delta F_{x.FR} = \Delta F_{x.RL} = \Delta F_{x.RR}$ * Priority Distribution in Region 1
Neg. $M_{z.tar}$ (-)	Case 5 (F_{yf}+, F_{yr}+)	$\Delta F_{x.RL} = \Delta F_{x.RR} \rightarrow \Delta F_{x.FL} = \Delta F_{x.FR}$ $0 \le \Delta F_{x.RL} \le max(0, -F_{x.RL})$ & $min(0, -F_{x.RR}) \le \Delta F_{x.RR} \le 0$
	Case 6 (F_{yf}-, F_{yr}+)	$\Delta F_{x.FL} = \Delta F_{x.FR} = \Delta F_{x.RL} = \Delta F_{x.RR}$ * Priority Distribution in Region 1
	Case 7 (F_{yf}-, F_{yr}-)	$\Delta F_{x.FL} = \Delta F_{x.FR} \rightarrow \Delta F_{x.RL} = \Delta F_{x.RR}$ $0 \le \Delta F_{x.FL} \le max(0, -F_{x.FL})$ & $min(0, -F_{x.FR}) \le \Delta F_{x.FR} \le 0$
	Case 8 (F_{yf}+, F_{yr}-)	$\Delta F_{x.FL} = \Delta F_{x.FR} = \Delta F_{x.RL} = \Delta F_{x.RR}$

Table 1 shows the optimal distribution strategies for each of the eight driving situations.

C. OPTIMIZATION

Based on the optimal distribution strategies for each driving situation derived in the previous section, the optimization module was developed. In optimization design, we are considering the optimal distribution strategy, the minimizing deceleration performance which is one of the goals of the distributor, and the limit torques of the motors. In the case of braking force, not only motor braking but also hydraulic braking can be used, so a limit on the braking force available is not considered. From now on, we will describe the optimization module in situations where the target yaw moment is positive. Prior to the design of the optimization module, we must perform unit conversion for the signals received as torque since the optimization module was designed based on the tire forces. The motor drive and hydraulic braking torque of each wheel that is output from the base logic of the braking/driving module and the traction limit torque of the

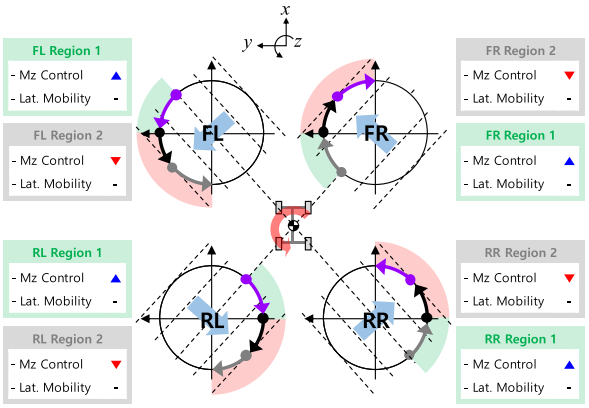

FIGURE 10. Control performance analysis result for Case 4.

motor can be converted into units of force as follows.

$$F_{x.Base.i} = \frac{\left(T_{q.Base.M.i} + T_{q.Base.H.i}\right)}{R_{Wheel}}$$
$$F_{x.Max.M.j} = \frac{T_{q.Max.M.j}}{R_{Wheel}} \quad (5)$$

where, i = FL, FR, RL, RR and j = FR, RR.

The first equation in (5) is the current longitudinal tire force of each wheel, the second equation represents the traction force limit of the motor for the FR and RR wheels.

1) CASE 1: $M_z > 0, F_{yf} > 0, F_{yr} > 0$

If the tire forces of the FL wheel and FR wheel are in Region 1, the target yaw moment is achieved by first distributing a braking force to the FL wheel and a driving force to the FR wheel. If the yaw moment generated by these is still insufficient, the insufficient yaw moment is achieved by distributing a braking force to the RL wheel and a driving force to the RR wheel. Therefore, the optimal distribution problem for Case 1 can be stated as follows:

$$L = q_1 \left\{ M_{z,tar} + \frac{t}{2} \begin{pmatrix} \Delta F_{x.FL.*} - \Delta F_{x.FR.*} \\ + \Delta F_{x.RL.*} - \Delta F_{x.RR.*} \end{pmatrix} \right\}^2 + q_2 \left(\sum_{\substack{i=FL,FR,\\ RL,RR}} \Delta F_{x.i.*} \right)^2 + \sum_{j=RL,RR} r_j \Delta F_{x.j.*}{}^2$$
$$subject\ to\ -\max\left(0, F_{x.Base.FL}\right) \le \Delta F_{x.FL.*} \le 0$$
$$0 \le \Delta F_{x.FR.*} \le -\min\left(0, F_{x.Base.FR}\right)$$
$$\Delta F_{x.RR.*} \le F_{x.Max.M.RR} - F_{x.Base.RR} \quad (6)$$

where, * indicates CASE 1; q_1, q_2, and r_j ($j = RL, RR$) are weighting factors.

The first and second terms of the cost function represent yaw moment tracking performance and deceleration minimization performance, respectively. The third term is to prioritize distribution of braking force of the FL wheel and driving force of the FR wheel under out optimal distribution strategy. The first and second constraint equations indicate the range of forces capable of using the FL braking force and FR driving force, respectively. The last constraint equation is a condition that considers the traction limit torque of the motor for the RR wheel. As shown in Fig. 5, there is no need to consider the traction limit torque of the motor for the FR wheel, since it is distributed only in Region 1.

2) CASE 2: $M_z > 0, F_{yf} < 0, F_{yr} > 0$

In Case 2, since all four wheels are effective in yaw moment tracking performance, the target yaw moment is achieved by optimally distributing forces to each wheel in proportion to the weight on each wheel. (7) shows the optimal distribution problem in Case 2.

$$L = q_1 \left\{ M_{z,tar} + \frac{t}{2} \begin{pmatrix} \Delta F_{x.FL.*} - \Delta F_{x.FR.*} \\ + \Delta F_{x.RL.*} - \Delta F_{x.RR.*} \end{pmatrix} \right\}^2 + q_2 \left(\sum_{\substack{i=FL,FR,\\ RL,RR}} \Delta F_{x.i.*} \right)^2 + \sum_{\substack{j=FL,FR,\\ RL,RR}} \left(\frac{\Delta F_{x.j.*}}{F_{z.j}} \right)^2$$
$$subject\ to\ \Delta F_{x.FR.*} \le F_{x.Max.M.FR} - F_{x.Base.FR}$$
$$\Delta F_{x.RR.*} \le F_{x.Max.M.RR} - F_{x.Base.RR} \quad (7)$$

where * indicates CASE 2.

In the same way as Case 1, the first and second terms of the cost function represent yaw moment tracking performance and deceleration minimization performance, respectively. The terms after the third term are there to distribute forces in proportion to the weight on each wheel to achieve the target yaw moment. The constraint equations consider the traction limit torques of the motors for the FR and RR wheels.

3) CASE 3: $M_z > 0, F_{yf} < 0, F_{yr} < 0$

The optimal distribution problem for Case 3 can be expressed as follows by swapping the front and rear wheels from Case 1.

$$L = q_1 \left\{ M_{z,tar} + \frac{t}{2} \begin{pmatrix} \Delta F_{x.FL.*} - \Delta F_{x.FR.*} \\ + \Delta F_{x.RL.*} - \Delta F_{x.RR.*} \end{pmatrix} \right\}^2 + q_2 \left(\sum_{\substack{i=FL,FR,\\ RL,RR}} \Delta F_{x.i.*} \right)^2 + \sum_{j=FL,FR} r_j \Delta F_{x.j.*}{}^2$$
$$subject\ to\ -\max\left(0, F_{x.Base.RL}\right) \le \Delta F_{x.RL.*} \le 0$$
$$0 \le \Delta F_{x.RR.*} \le -\min\left(0, F_{x.Base.RR}\right)$$
$$\Delta F_{x.FR.*} \le F_{x.Max.M.FR} - F_{x.Base.FR} \quad (8)$$

4) CASE 4: $M_z > 0, F_{yf} > 0, F_{yr} < 0$

The distribution strategy in Case 4 is to first achieve the target yaw moment by distributing forces to the wheels where the current tire force is in Region 1. After this if the yaw moment generated is still insufficient, the insufficient yaw moment is achieved by distributing appropriate forces considering the controllable margin of each wheel. The controllable margin refers to the amount of the braking or driving force to be added at each wheel that can move the tire force to just before the yaw moment adverse effect region, as shown in Fig. 10.

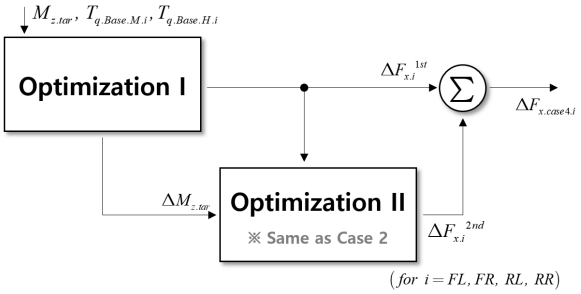

FIGURE 11. Structure of the optimal distribution algorithm for Case 4.

Fig. 11 shows the structure of the optimal distribution algorithm for Case 4. This structure is made up of Optimization I for priority distribution in Region 1 and Optimization II for the distribution of forces in proportion to the controllable margin. The optimal forces to be distributed to each wheel in Case 4 are determined by summing the outputs of Optimization I and Optimization II modules.

The optimal distribution problem in Optimization I can be expressed as follows.

$$\begin{aligned} L = {} & q_1 \left\{ M_{z,tar} + \frac{t}{2} \left(\begin{array}{c} \Delta F_{x.FL}^{1st} - \Delta F_{x.FR}^{1st} \\ + \Delta F_{x.RL}^{1st} - \Delta F_{x.RR}^{1st} \end{array} \right) \right\}^2 \\ & + \sum_{j=FL,FR,RL,RR} r_j \left(\Delta F_{x.j}^{1st} \right)^2 \\ & subject\ to \ -\max\left(0, F_{x.Base.FL}\right) \le \Delta F_{x.FL}^{1st} \le 0 \\ & 0 \le \Delta F_{x.FR}^{1st} \le -\min\left(0, F_{x.Base.FR}\right) \\ & -\max\left(0, F_{x.Base.RL}\right) \le \Delta F_{x.RL}^{1st} \le 0 \\ & 0 \le \Delta F_{x.RR}^{1st} \le -\min\left(0, F_{x.Base.RR}\right) \end{aligned} \quad (9)$$

The constraint equations in (9) relate to Region 1 for each wheel. For all four wheels, Region 1 includes a longitudinal tire force of up to 0, so the traction limit torque of the motor is not considered. From the results of (9), the insufficient yaw moment can be calculated as follows.

$$\Delta M_z = M_{z,tar} + \frac{t}{2} \left(\Delta F_{x.FL}^{1st} - \Delta F_{x.FR}^{1st} + \Delta F_{x.RL}^{1st} - \Delta F_{x.RR}^{1st} \right) \quad (10)$$

Optimization II module is used to generate the yaw moment in (10). As mentioned above, it should be distributed so that the tires forces move stop just before entering the yaw moment adverse effect region. To do this, the controllable margin of each wheel must first be calculated. Fig. 12 shows the limit for longitudinal tire forces on the FL wheel that generate the maximum yaw moment. These can be obtained from the tire-road friction coefficient, the vertical force, and the slope of the yaw moment contour line.

The longitudinal tire force limits of the remaining wheels can be calculated as follows by applying the same method.

$$\begin{aligned} F_{x.Mz.Lim.FL} &= -\mu F_{z.FL} \cos\theta_1 \\ F_{x.Mz.Lim.FR} &= \mu F_{z.FR} \cos\theta_1 \\ F_{x.Mz.Lim.RL} &= -\mu F_{z.RL} \cos\theta_2 \\ F_{x.Mz.Lim.RR} &= \mu F_{z.RR} \cos\theta_2 \end{aligned}$$

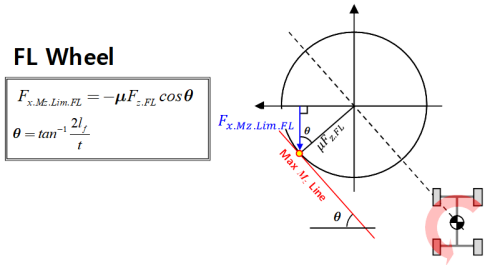

FIGURE 12. Limit longitudinal tire force of the FL wheel.

$$where,\ \theta_1 = \frac{2l_f}{t}, \quad \theta_2 = \frac{2l_r}{t} \quad (11)$$

Using (10) and (11), the controllable margin of each wheel can be calculated.

$$\begin{aligned} F_{x.FL.\mathrm{Mar}} &= \min\left(0, \quad F_{x.Mz.Lim.FL} - F_{x.Base.FL} - \Delta F_{x.FL}^{1st}\right) \\ F_{x.FR.\mathrm{Mar}} &= \max\left(0, \begin{array}{c} \min\left(F_{x.Mz.Lim.FR}, F_{x.Max.M.FR}\right) \\ - F_{x.Base.FR} - \Delta F_{x.FR}^{1st} \end{array}\right) \\ F_{x.RL.\mathrm{Mar}} &= \min\left(0, \quad F_{x.Mz.Lim.RL} - F_{x.Base.RL} - \Delta F_{x.RL}^{1st}\right) \\ F_{x.RR.\mathrm{Mar}} &= \max\left(0, \begin{array}{c} \min\left(F_{x.Mz.Lim.RR}, F_{x.Max.M.RR}\right) \\ - F_{x.Base.RR} - \Delta F_{x.RR}^{1st} \end{array}\right) \end{aligned} \quad (12)$$

Since the FR and RL wheels are being driven, the controllable margins for those wheels must take into account the traction torque limit of the motor. Using (12), the optimal distribution problem from Optimization II can be expressed as follows.

$$\begin{aligned} L = {} & q_1 \left\{ \Delta M_z + \frac{t}{2} \left(\begin{array}{c} \Delta F_{x.FL}^{2nd} - \Delta F_{x.FR}^{2nd} \\ + \Delta F_{x.RL}^{2nd} - \Delta F_{x.RR}^{2nd} \end{array} \right) \right\}^2 \\ & + q_2 \left\{ \sum_{\substack{i=FL,FR,\\ RL,RR}} \left(\Delta F_{x.i}^{1st} + \Delta F_{x.i}^{2nd} \right) \right\}^2 \\ & + \sum_{\substack{i=FL,FR,\\ RL,RR}} \left(\frac{\Delta F_{x.i}^{2nd}}{F_{x.i.\mathrm{Mar}}} \right)^2 \\ & subject\ to\ F_{x.FL.\mathrm{Mar}} \le \Delta F_{x.FL}^{2nd} \le 0 \\ & 0 \le \Delta F_{x.FR}^{2nd} \le F_{x.FR.\mathrm{Mar}} \\ & F_{x.RL.\mathrm{Mar}} \le \Delta F_{x.RL}^{2nd} \le 0 \\ & 0 \le \Delta F_{x.RR}^{2nd} \le F_{x.RR.\mathrm{Mar}} \end{aligned} \quad (13)$$

The second term of the cost function shows the deceleration minimization performance. Optimization I does not consider deceleration minimization performance, so it is necessary to compensate for this. By summing the results of Optimization I and Optimization II, the forces distributed to each wheel in Case 4 can be determined as follows.

$$\begin{aligned} \Delta F_{x.FL.CASE4} &= \Delta F_{x.FL}^{1st} + \Delta F_{x.FL}^{2nd} \\ \Delta F_{x.FR.CASE4} &= \Delta F_{x.FR}^{1st} + \Delta F_{x.FR}^{2nd} \\ \Delta F_{x.RL.CASE4} &= \Delta F_{x.RL}^{1st} + \Delta F_{x.RL}^{2nd} \\ \Delta F_{x.RR.CASE4} &= \Delta F_{x.RR}^{1st} + \Delta F_{x.RR}^{2nd} \end{aligned} \quad (14)$$

5) FINAL DISTRIBUTED OPTIMAL FORCE

So far, the optimal forces distributed to each wheel have been determined in the four cases where the target yaw moment is positive. From these outputs, the final forces distributed to each wheel can be calculated simply by changing the results for each case according to the sign of the lateral tire force of the front and rear wheels. However, when the sign of the lateral tire force changes, the final forces change discretely. Also, the optimal distribution strategy is not valid when the tire lateral force is small, since this strategy was established under the assumption that the tire lateral force is large. If the lateral tire force is small, all wheels have the same control effect, because the lateral tire force changes according to the longitudinal tire force changes are small. Therefore, the final forces are determined by the sum of the weights as follows.

$$\begin{aligned}&\Delta F_{x.i}\\&= w_r\left\{w_f\Delta F_{x.i.CASE1}+\left(1-w_f\right)\Delta F_{x.i.CASE2}\right\}\\&\quad+\left(1-w_r\right)\left\{\left(1-w_f\right)\Delta F_{x.i.CASE3}+w_f\Delta F_{x.i.CASE4}\right\}\end{aligned}\quad(15)$$

where, i = FL, FR, RL, RR.

w_f and w_r are the weighting factors used according to the signs of the lateral tire forces on the front and rear wheels, respectively. As shown in Fig. 13, it can be seen that the range of this lateral tire force, which goes from $-F_{yf.threshold}(-F_{yr.threshold})$ to $F_{yf.threshold}(F_{yr.threshold})$, is defined as a transition area and the weighting factors are determined to change linearly. $F_{yf.threshold}$ *and* $F_{yr.threshold}$ can be determined by tuning through experiments. From (15) and Fig. 13, when the lateral tire forces on the front and rear wheels are both zero, it can be seen that the final force is calculated as the average of the forces determined in 4 cases.

Looking at the architecture shown in Fig.1, the final output of the optimization module is torque. This is calculated by multiplying the result of (15) by the tire radius.

$$\Delta T_{q.i}=R_{Wheel}\Delta F_{x.i},\quad Where,\ i=FL,FR,RL,RR\quad(16)$$

D. BLENDING

The blending module distributes the torque of each wheel calculated by the optimization module as motor torque and hydraulic torque. The motor torque and hydraulic torque are determined in a way that maximizes the regenerative braking of the motor in consideration of fuel economy as follows.

$$\begin{aligned}&if\ \Delta T_{q.i}<0\\&\Delta T_{q.M.i}=\max\left\{\Delta T_{q.i},\min\left(0,T_{q.Min.M.i}-T_{q.Base.M.i}\right)\right\}\\&\Delta T_{q.H.i}=\Delta T_{q.i}-\Delta T_{q.M.i}5\\&else\\&\Delta T_{q.H.i}=\min\left(\Delta T_{q.i},-T_{q.Base.H.i}\right)\\&\Delta T_{q.M.i}=\Delta T_{q.i}-\Delta T_{b.H.i}\end{aligned}\quad(17)$$

If the additional torque to be distributed is negative and regenerative braking of the motor is possible, torque is first distributed as braking of the motor, any extra braking torque needed is distributed as hydraulic braking. Conversely, if the additional torque to be distributed is positive and hydraulic braking is underway, reducing this hydraulic braking is prioritized.

TABLE 2. Parameters of the CarSim vehicle model.

Parameter	Value
Total vehicle mass	2041.2 kg
Moment of inertia about roll axis (I_x)	660 $kg{\cdot}m^2$
Moment of inertia about pitch axis (I_y)	2989 $kg{\cdot}m^2$
Moment of inertia about yaw axis (I_z)	3174 $kg{\cdot}m^2$
Distance from C.G to front axle (l_f)	1.4495 m
Distance from C.G to rear axle (l_r)	1.5105 m
Radius of wheel (R_{Wheel})	0.353 m
Tread (track width) (t)	1.661 m
Tire model (Pacejka tire model)	225/60 R18

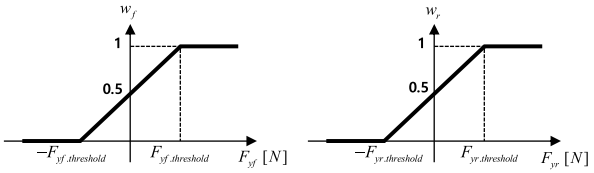

FIGURE 13. Weighting factors (w_f, w_r).

V. EVALUATION

The proposed control logic was evaluated through computer simulations using CarSim and MATLAB/Simulink. CarSim is vehicle simulation software, and the proposed control logic is implemented within the MATLAB/Simulink environment. The parameters of the CarSim vehicle model are given Table 2. The power and the reduction ratio of the motor mounted at each wheel is 60KW and 12.9, respectively. Fig. 14 is the characteristic torque curve of the motor, showing the maximum and minimum torques with respect to motor speed.

The following two simulations were conducted to test the effectiveness of the proposed control system: 1) an open-loop sine maneuver simulation to evaluate the yaw moment control performance and the deceleration minimization performance and 2) an acceleration and turning simulation to evaluate lateral movement performance. The proposed algorithm was compared with results of a ESC system and a conventional optimization method. The ESC system uses only differential braking, and the conventional optimization is the method that optimally distributes braking and driving forces in proportion to the load on each wheel. In these simulations, the steering wheel angle was determined by a driver steering model that imitates human drivers' steering behavior in lane-following situations. This model is provided in the Carsim software.

A. OPEN-LOOP SINE MANEUVER SIMULATION

To evaluate the yaw moment control performance and the deceleration minimization performance, an open-loop sine

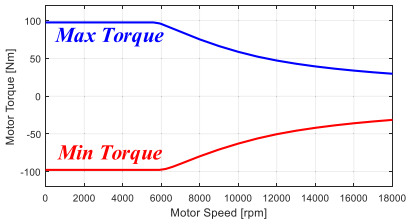

FIGURE 14. Motor characteristics.

maneuver was simulated on asphalt road. The initial vehicle speed was set to 120 km/h, and no throttle input was applied during the simulation. Fig. 15 shows the simulation results. Fig. 15(a)-(d) show the steering wheel angle, yaw rate, velocity, and control inputs to the motors and hydraulics, respectively. The black solid line, red solid line, and blue dotted line represent the resuslts of the ESC system, conventional optimization method, and proposed method, respectively. In Fig. 15(b), the proposed method shows that the yaw moment performance is slightly improved compared to the conventional optimization method. In the case of the ESC system, it shows the different performance than the other two methods because only hydraulic braking, which has a slower response speed than the motor, is used. However, it can be seen that all methods guarantee the lateral stability of the vehicle. The deceleration minimization performance results are shown in Fig. 15(c). When the proposed method and conventional optimization method are applied, the vehicle speed remains approximately 20 km/h higher than with the ESC system. This result can be explained by looking at the control input results in Fig. 15(d). In the case of the ESC system, only hydraulic braking was used, resulting in significant deceleration, however, with the proposed method and conventional optimization method, the deceleration is minimized by using both the driving force and braking force of the motor at the same time.

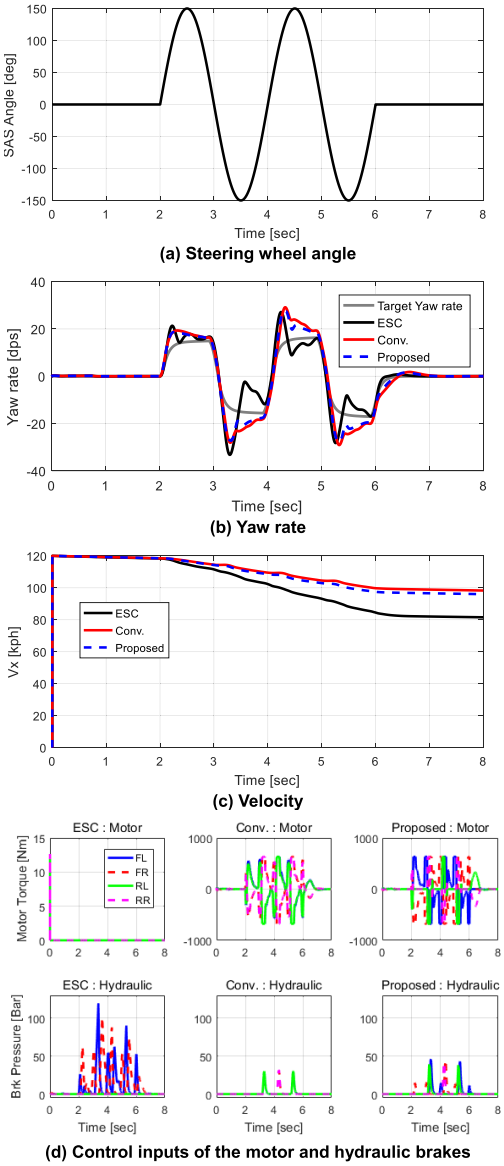

FIGURE 15. Simulation results for open-loop sine maneuver.

B. ACCELERATION-TURNING SIMULATION

To evaluate the lateral movement performance, the acceleration and turning maneuvers were simulated on a snow covered road (mu = 0.4), as shown Fig. 16. The initial vehicle speed was set to 5 km/h, 20% throttle input was then applied from the 1 second. To clearly show the control effects, the acceleration torque due to throttle input was only applied to the rear wheels. In the test, to turn left, the driver turns the steering wheel counterclockwise. Since the acceleration torque is applied only to the rear wheel, oversteer occurs during turning. That is, this test scenario is the same situation as Case 5 in Table 1.

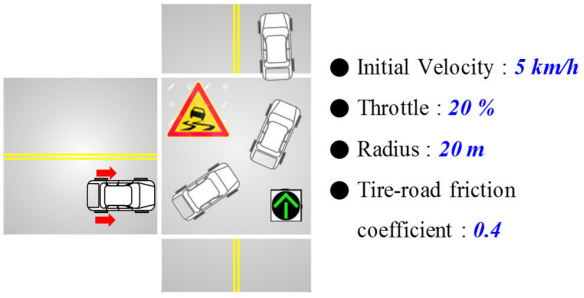

FIGURE 16. Acceleration-turning test on snow road.

Fig. 17 shows the simulation results for the acceleration and turning test. Fig. 17(a)-(e) show the steering wheel angle, yaw rate, velocity, lateral acceleration, and trajectory, respectively. It can be seen from Fig. 17(a) and (b) that the steering wheel angle for tracking the reference trajectory and the yaw rate generated by the steering wheel angle and the lateral stability control are similar in both the conventional optimal method and the proposed method. In Fig. 17(d), the lateral acceleration of the proposed method is larger than that of the conventional optimal method because the proposed logic distributes the wheel forces by considering not only the yaw moment control performance but also the lateral movement performance. As a result, it can be seen from Fig. 17(e) that the trajectory tracking performance of the proposed logic is

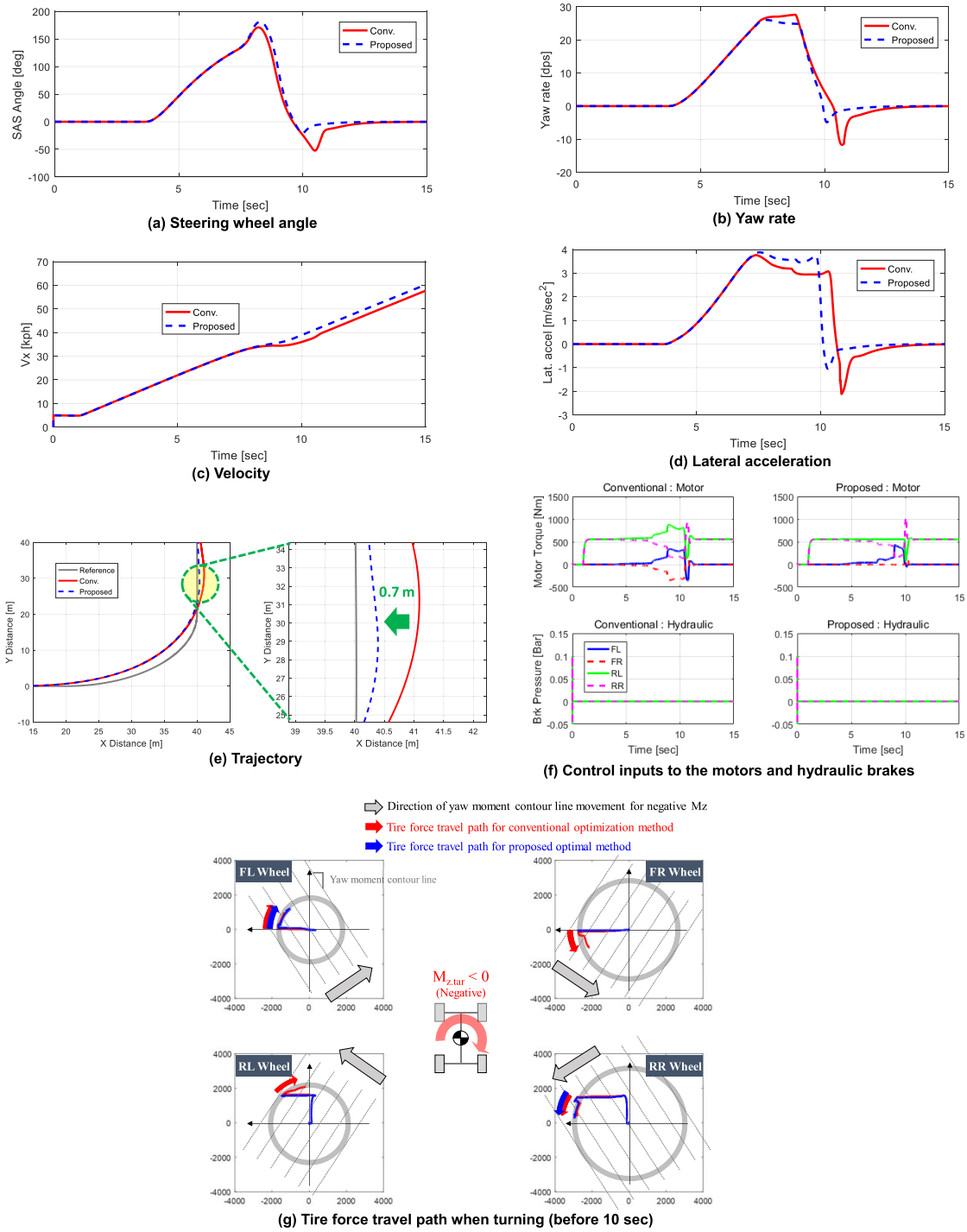

FIGURE 17. Simulation results for acceleration-turning test.

superior. Fig. 17(f) and (g) show the control inputs and the tire force travel path at each wheel according to these control inputs, respectively. In Fig. 17(f), when turning (before 10 sec), the conventional optimization method distributes the braking force and driving force evenly to the 4 wheels, while the proposed method shows that the driving force and braking force are distributed to FL and RR, respectively. The tire force travel path at each wheel according to these control inputs can be seen in Fig. 17(g). The conventional optimization method additionally uses the braking of the FR wheel and the driving of the RL wheel. Here, in the case of the FR wheel braking, the yaw moment control effect is good because it moves the yaw moment contour line in the negative direction. However, the lateral movement performance is poor because the lateral force is reduced. In the case of the RL wheel driving, it moves the yaw moment contour line in the positive direction. This is in the opposite direction to the target yaw moment, and the yaw moment control performance is very poor. The lateral

force is also greatly reduced, so the lateral movement performance is also poor. In other words, the yaw moment control effect caused by FR braking is canceled by RL driving. Also, due to these two control inputs, the lateral tire forces are reduced. Therefore, both the conventional optimization method and the proposed method show similar performance in terms of the lateral stability, but the proposed method is superior in terms of the lateral movement performance.

VI. CONCLUSION

A new algorithm that independently controls braking and driving forces at each wheel to improve the lateral stability of a vehicle equipped with independent-drive motors at all wheels was proposed. The proposed control algorithm controls the yaw rate to track the target yaw rate using driving or braking forces to each of the 4 wheels. This is approach is quite similar to previous research. The algorithm is made up of a target yaw rate, Mz controller and distributor. The target yaw rate and Mz controller were designed using the results of previous research, while the distributor is new. In order to develop this new distribution logic, the concept of a yaw moment contour line was introduced, using this concept, optimal distribution strategies in consideration of yaw moment control performance, lateral movement performance, and deceleration minimization performance for all possible driving situations (8 cases) were developed. These optimal distribution strategies are the main contribution of this paper. Based on these distribution strategies, an optimization module for the distributor was designed, the final torques applied to the motors and the hydraulic brakes were determined using a blending module. Computer simulations were conducted to verify the proposed control algorithm. From the simulation results, it was verified that the proposed algorithm improves not only yaw moment control performance but also lateral movement performance and deceleration minimization performance.

The optimization module developed in this paper has to solve a total of 8 optimization problems with constraints. These problems were solved in MATLAB using fmincon functions. These occurs an iterative computation which aggravates the real-time computation. Therefore, our future research is to improve the distribution logic to secure real-time computation, and to verify the performance of the proposed logic through actual vehicle testing.

APPENDIX

Nomenclature list:

g	Acceleration due to gravity.
l_f	Distance from CG to front axle.
l_r	Distance from CG to rear axle.
t	Track width.
C_f	Front tire cornering stiffness.
C_r	Rear tire cornering stiffness.
i	1, 2, 3, and 4 corresponding to front left, front right, rear left, and rear right (=FL, FR, RL, RR).
$*$	1, 2, 3, and 4 corresponding to CASE 1, CASE 2, CASE 3, and CASE 4.
$F_{x.i}$	Longitudinal tire force at the ith tire.
$F_{x.Base.i}$	Longitudinal tire force, is generated by the base logic for braking/driving module, at the ith tire.
$F_{x.Max.M.i}$	Maximum driving tire force, can be generated by the motor of the ith wheel.
F_{yf}	Front lateral tire force.
F_{yr}	Rear lateral tire force.
I_z	Moment of inertia about the yaw axis.
$M_{z.tar}$	Target yaw moment.
R_{Wheel}	Effective radius of the wheel.
$T_{q.Base.M.i}$	Motor torque, is calculated by the base logic for braking/driving module, at the ith tire.
$T_{q.Base.H.i}$	Hydraulic braking torque, is calculated by the base logic for braking/driving module, at the ith tire.
$T_{q.Max.M.i}$	Maximum driving torque, can be generated by the motor of the ith wheel.
$T_{q.Min.M.i}$	Maximum braking torque, can be generated by the motor of the ith wheel.
V_x	Longitudinal velocity at CG.
$\Delta F_{x.i}$	Additional longitudinal tire force, is calculated by the optimization, at ith tire.
$\Delta F_{x.i.*}$	Additional longitudinal tire force, is calculated by the optimization, at the ith tire for each case.
$\Delta T_{q.i}$	Total torque (motor + hydraulic brake), is calculated by the optimization, applied to the ith tire.
$\Delta T_{q.M.i}$	Motor torque calculated by the blending, applied to the ith tire.
$\Delta T_{q.H.i}$	Hydraulic brake torque calculated by the blending, applied to the ith tire.
β	Vehicle side slip angle.
δ_f	Front steering angle.
γ	Yaw rate.
γ_t	Target yaw rate.
μ	Tire-road friction coefficient.

REFERENCES

[1] Bloomberg New Energy Finance. *Electric Vehicle Output 2020*. USA. Accessed: Jan. 28, 2021. [Online]. Available: http:// https://about.bnef.com/electric-vehicle-outlook

[2] J. Kang, J. Yoo, and K. Yi, "Driving control algorithm for maneuverability, lateral stability, and rollover prevention of 4WD electric vehicles with independently driven front and rear wheels," *IEEE Trans. Veh. Technol.*, vol. 60, no. 7, pp. 2987–3001, Sep. 2011.

[3] Y. Chen, S. Chen, Y. Zhao, Z. Gao, and C. Li, "Optimized handling stability control strategy for a four in-wheel motor independent-drive electric vehicle," *IEEE Access*, vol. 7, pp. 17017–17032, 2019, doi: 10.1109/ACCESS.2019.2893894.

[4] J. Wang, Z. Luo, Y. Wang, B. Yang, and F. Assadian, "Coordination control of differential drive assist steering and vehicle stability control for four-wheel-independent-drive EV," *IEEE Trans. Veh. Technol.*, vol. 67, no. 12, pp. 11453–11467, Dec. 2018.

[5] K. Nam, H. Fujimoto, and Y. Hori, "Lateral stability control of in-wheel-motor-driven electric vehicles based on sideslip angle estimation using lateral tire force sensors," *IEEE Trans. Veh. Technol.*, vol. 61, no. 5, pp. 1972–1985, Jun. 2012.

[6] M. Yue, L. Yang, X.-M. Sun, and W. Xia, "Stability control for FWID-EVs with supervision mechanism in critical cornering situations," *IEEE Trans. Veh. Technol.*, vol. 67, no. 11, pp. 10387–10397, Nov. 2018.

[7] R. Hou, L. Zhai, T. Sun, Y. Hou, and G. Hu, "Steering stability control of a four in-wheel motor drive electric vehicle on a road with varying adhesion coefficient," *IEEE Access*, vol. 7, pp. 32617–32627, 2019, doi: 10.1109/ACCESS.2019.2901058.

[8] D.-H. Kim, J.-M. Kim, S.-H. Hwang, and H.-S. Kim, "Optimal brake torque distribution for a four-wheeldrive hybrid electric vehicle stability enhancement," *Proc. Inst. Mech. Eng., D, J. Automobile Eng.*, vol. 221, no. 11, pp. 1357–1366, Nov. 2007.

[9] Z. Shuai, H. Zhang, J. Wang, J. Li, and M. Ouyang, "Combined AFS and DYC control of four-wheel-independent-drive electric vehicles over CAN network with time-varying delays," *IEEE Trans. Veh. Technol.*, vol. 63, no. 2, pp. 591–602, Feb. 2014.

[10] S. Yim, J. Choi, and K. Yi, "Coordinated control of hybrid 4WD vehicles for enhanced maneuverability and lateral stability," *IEEE Trans. Veh. Technol.*, vol. 61, no. 4, pp. 1946–1950, May 2012.

[11] R. Wang, C. Hu, Z. Wang, F. Yan, and N. Chen, "Integrated optimal dynamics control of 4WD4WS electric ground vehicle with tire-road frictional coefficient estimation," *Mech. Syst. Signal Process*, vols. 60–61, pp. 727–741, Aug. 2015.

[12] Q. Wang, Y. Zhao, Y. Deng, H. Xu, H. Deng, and F. Lin, "Optimal coordinated control of ARS and DYC for four-wheel steer and in-wheel motor driven electric vehicle with unknown tire model," *IEEE Trans. Veh. Technol.*, vol. 69, no. 10, pp. 10809–10819, Oct. 2020.

[13] H. Fujimoto and K. Maeda, "Optimal yaw-rate control for electric vehicles with active front-rear steering and four-wheel driving-braking force distribution," in *Proc. 39th Annu. Conf. IEEE Ind. Electron. Soc. (IECON)*, Nov. 2013, pp. 6514–6519.

[14] E. Ono, Y. Hattori, Y. Muragishi, and K. Koibuchi, "Vehicle dynamics integrated control for four-wheel-distributed steering and four-wheel-distributed traction/braking systems," *Vehicle Syst. Dyn.*, vol. 44, no. 2, pp. 139–151, Feb. 2006.

[15] A. Goodarzi and M. Alirezaie, "A new fuzzy-optimal integrated AFS/DYC control strategy," in *Proc. AVEC*, 2006, pp. 65–70.

[16] J. Ni, J. Hu, and C. Xiang, "Envelope control for four-wheel independently actuated autonomous ground vehicle through AFS/DYC integrated control," *IEEE Trans. Veh. Technol.*, vol. 66, no. 11, pp. 9712–9726, Nov. 2017.

[17] W. Cho, J. Choi, C. Kim, S. Choi, and K. Yi, "Unified chassis control for the improvement of agility, maneuverability, and lateral stability," *IEEE Trans. Veh. Technol.*, vol. 61, no. 3, pp. 1008–1020, Mar. 2012.

[18] R. Kazemi, J. Ahmadi, A. Ghaffari, and M. Kabganian, "Vehicle yaw stability control through combined differential braking and active rear steering based on linguistic variables," in *Proc. AVEC*, 2006, pp. 661–666.

[19] S.-H. You, J.-S. Jo, S. Yoo, J.-O. Hahn, and K. I. Lee, "Vehicle lateral stability management using gain-scheduled robust control," *J. Mech. Sci. Technol.*, vol. 20, no. 11, pp. 1898–1913, Nov. 2006.

[20] W. Cho, J. Yoon, S. Yim, B. Koo, and K. Yi, "Estimation of tire forces for application to vehicle stability control," *IEEE Trans. Veh. Technol.*, vol. 59, no. 2, pp. 638–649, Feb. 2010.

[21] J. J. Rath, K. C. Veluvolu, and M. Defoort, "Simultaneous estimation of road profile and tire road friction for automotive vehicle," *IEEE Trans. Veh. Technol.*, vol. 64, no. 10, pp. 4461–4471, Oct. 2015.

[22] M. U. Cuma and T. Koroglu, "A comprehensive review on estimation strategies used in hybrid and battery electric vehicles," *Renew. Sustain. Energy Rev.*, vol. 42, pp. 517–531, Feb. 2015, doi: 10.1016/j.rser.2014.10.047.

[23] X. Jin, J. Yang, Y. Li, B. Zhu, J. Wang, and G. Yin, "Online estimation of inertial parameter for lightweight electric vehicle using dual unscented Kalman filter approach," *IET Intell. Transp. Syst.*, vol. 14, no. 5, pp. 412–422, 2020.

IN-GYU JANG received the B.S. and M.S. degrees in mechanical engineering from Sungkyunkwan University, Suwon, South Korea, in 2004 and 2008, respectively, where he is currently pursuing the Ph.D. degree with the School of Mechanical Engineering. His research interests include integrated chassis control systems, electrified powertrain control systems, and motion control systems for future e-mobility solutions.

SEUNG-HAN YOU received the B.S., M.S., and Ph.D. degrees in mechanical and aerospace engineering from Seoul National University, Seoul, South Korea, in 1999, 2001, and 2006, respectively. From 2006 to 2015, he was a Senior Research Engineer with the Automotive Research and Development Division, Hyundai Motor Group, Gyeonggi-do, South Korea. Since 2015, he has been with the School of Mechanical Engineering, Korea University of Technology and Education, where he is currently an Associate Professor. His current research interests include control systems, state estimations, parameter estimations, and their applications in future vehicles.

SUNG-HO HWANG received the B.S., M.S., and Ph.D. degrees in mechanical design and production engineering from Seoul National University, Seoul, South Korea, in 1988, 1990, and 1997, respectively.

From 1992 to 2002, he was a Senior Researcher with Korea Institute of Industrial Technology, Cheonan. Since 2002, he has been a Professor with the School of Mechanical Engineering, Sungkyunkwan University, Suwon, South Korea. He is the author of two books, more than 100 articles, and more than 20 inventions. His research interests include fundamental problems of dynamic systems, measurements, and control in automotive applications, such as powertrain systems, electronically controlled chassis systems, and electric drive systems among others.

Prof. Hwang served as the Editor-in-Chief for the *Journal of Drive and Control*, from 2012 to 2016. He was the Vice-President of the Korean Society of Automotive Engineers (KSAE), in 2021.

WANKI CHO received the B.S. degree in mechanical engineering from Hanyang University, Seoul, South Korea, in 2004, and the M.S. and Ph.D. degrees in mechanical and aerospace engineering from Seoul National University, Seoul, in 2006 and 2011, respectively. From 2011 to 2019, he was a Senior Research Engineer with the Automotive Research and Development Division, Hyundai Motor Group, Gyeonggi-do, South Korea. Currently, he is an Assistant Professor with the School of Mechanical Engineering, Korea University of Technology and Education. His research interests include integrated chassis control systems and intelligent vehicle control.